Reports on Geodesy and Geoinformatics, 2026, Vol. 121, pp. 59–66

DOI: 10.2478/rgg-2026-0005
Received: 21 July 2025 / Accepted: 15 April 2026
Published online: 15 May 2026

ORIGINAL ARTICLE

A practical approach to coupling GNSS and precise geometric leveling

Baryła Radosław [1*] and Ogrodniczak Michał [1]

[1]Department of Geodesy, University of Warmia and Mazury in Olsztyn, Oczapowskiego 2, 10-719, Olsztyn, Poland

*radoslaw.baryla@uwm.edu.pl

Abstract

This study aims to couple satellite data with precise geometric models. The performance assessment of the method is based on the dataset collected at a part of the vertical base geodetic control network in the Podkarpackie province in Poland. We used baselines determined in two 12-hour-long static Global Navigation Satellite System (GNSS) measurement sessions and reference coordinates of vertical base points of the geodetic control network. Baselines obtained from satellite measurements were used for the fusion, considering the height anomalies taken from the corresponding official geoid model PL-geoid2021. Proprietary solutions played a key role in satellite measurements by ensuring the correct performance of long-term measurements without requiring the manual measurement of the height of GNSS antennas relative to the marks of the measured geodetic control points. Two patented solutions were used for the first time in this study. The results confirmed the correctness and high applicability of the presented approach.

Key words: leveling, GNSS, geoid, control network, normal height

1 Introduction

Due to the deformations of the Earth's surface and the subsidence of vertical control network marks, the coordinates of the vertical control networks become out of date, so in Poland, it is recommended to conduct precision leveling of the entire basic vertical network every 20 years. The following precision leveling campaigns were conducted in Poland after the country regained independence (Kadaj, 2018; Wyrzykowski, 1993):

- 1926 – 1937: establishment of an accurate, uniform height network necessary for the economic development of the country,
- 1947 – 1955: supplementary work in the Recovered Territories, development of a new network linked with neighboring countries,
- 1974 – 1982: densification of the previous network, improvement of accuracy, linkage with mareographic stations, study of vertical movements of the Earth's crust, creation of a Unified Height Leveling Network (UHLN) with neighboring countries, further, based on the 1978 development of the "Concept for modernization of the country's vertical geodetic network",
- 1999 – 2002: implementation of a new height system, which is a mathematical and physical realization of the European Vertical Reference System (EVRS), a kinematic European vertical system adopting differences in gravity potential referenced to the Amsterdam reference level or corresponding normal heights, approved by Resolution No. 5 at the EUREF sub-committee assembly in Tromsø in 2000[1],
- 2024: commencement of the project implementation of the modernization of the basic height geodetic network.

The result of the first measurement campaign, in the years 1926–1937, was a vertical network referenced to the German Normal-Null level, which is the level of the North Sea in Amsterdam, represented by the benchmark placed on the Torun Town Hall (H = 50.518 m). The following measurement campaign in the first stage was aimed at extending the network established in the interwar period. In the second stage, a uniform network was measured throughout the country, which led to the establishment of a network referenced to the Baltic Sea level in Kronstadt (Wyrzykowski, 1993). Based

1 https://www.euref.eu/euref-symposia/troms%C3%B8-norway-22-24062000

on measurements from the 1950s, the state normal height system "Kronsztadt'1960" was defined. The third measurement campaign, in the years 1974–1982, consisted of two stages of development. In the first stage, the main focus was on updating the vertical coordinates of points that had become outdated as a result of vertical movements of the Earth's crust, densifying the class I leveling network, linking it to mareographic stations, and creating the UHLN together with neighboring states. In the second stage, in 1978, the "Concept of modernization of the country's vertical geodetic network" was developed, aimed at densifying the Polish fragment of the UHLN for economic reasons, attaching part of the class II tracts to the class I network. Based on this work, the new state vertical system "Kronsztadt'1986" was defined. The difference between these systems ($H^{Kr60} - H^{Kr86}$) oscillated between -0.012 m and 0.139 m. In practice, these systems were used in parallel even in the first decade of the 21st century, causing many problems in the implementation of projects, for example, roads, highways, and railways. The fifth measurement campaign of the height network was conducted in 1999 – 2002, which resulted in the creation of a new reference system "Kronsztadt'2006". Despite the high accuracy of point height determination, this system was not formally adopted for practical use. The main reason for this decision was the planned return to a uniform European vertical system for the mean level of the North Sea. Subsequently, in accordance with the recommendations of the European Commission in the Infrastructure for Spatial Information in Europe (INSPIRE) Directive (Journal of the European Union, 2010), data from the "Kronsztadt'2006" system were used to determine heights in the new PL-EVRF2007-NH datum, which is the Polish implementation of the European Vertical Reference Frame 2007 (EVRF2007), tied to mean sea level measured at the Amsterdam mareograph (Normal Amsterdam Peil – NAP) (Gajderowicz, 2007; Kadaj, 2018). Preparations are currently underway for the fifth precision leveling campaign, which will also use GNSS satellite measurements (Ogrodniczak et al., 2022).

2 Geometric leveling

Precise geometric leveling is aimed at updating the coordinates of points of the basic height control network that change due to movements of the Earth's crust or as a result of subsidence. It involves determining the height differences of points in the actual vector field of gravity. Since the mutual position of equipotential surfaces is irregular, calculation of the height of points of leveling tracts requires corrections to the height in the adopted height system, in addition to the vertical values obtained by the technique of precise geometric leveling. In Poland, a normal height system is implemented, in which the height differences ΔH^N_{AB} between adjacent points A and B are the sum of the measured height difference Δn_{AB} and the normal correction NC_{AB}. It can be written as:

$$\Delta H^N_{AB} = H^N_B - H^N_A = \Delta n_{AB} + NC_{AB}\,. \tag{1}$$

Normal correction NC_{AB}, calculated from the measured actual accelerations g, the calculated mean normal accelerations $\overline{\gamma}_A$ and $\overline{\gamma}_B$ at points A and B, and the normal accelerations γ_0 calculated on the reference ellipsoid (Heiskanen and Moritz, 1981), can be written as:

$$NC_{AB} = \sum_A^B \frac{g-\gamma_0}{\gamma_0}\delta n + \frac{\overline{\gamma}_A-\gamma_0}{\gamma_0}H^N_A - \frac{\overline{\gamma}_B-\gamma_0}{\gamma_0}H^N_B\,. \tag{2}$$

Normal corrections are calculated from gravimetric data (Barlik and Pachuta, 2007). Additionally, in precise leveling, at the stage of processing observation results in the form of height differences Δn_{AB}, the following phenomena with a direct impact on the measurement results during their implementation should be considered: comparative corrections of leveling rods, changes in the length of leveling rods caused by temperature variations during measurement, and diurnal variations in the direction of the plumb line caused by the gravity of the Sun and Moon. In addition, the comparative, thermal, and lunisolar corrections are incorporated in precision leveling (Journal of Laws of the Republic of Poland, 2021).

In the normal height system, corresponding to Molodiensky's theory, physical equipotential surfaces (actual vector gravitational field) are theoretically replaced by mathematical spheropotential surfaces (normal vector gravitational field). The normal height at a given point is calculated along the normal vertical line from the ellipsoid with normal potential U_0 equal to the actual potential of the geoid W_0, to the spheropotential surface U_P corresponding to the equipotential surface W_P containing point P located on the Earth's surface, where $U_P = W_P$ (Kamela et al., 1993).

3 GNSS leveling

Point coordinates obtained from GNSS measurements can be expressed in an orthogonal, Cartesian geocentric reference frame or as geodetic coordinates with respect to an ellipsoid inscribed in this system. The ellipsoidal heights of points are determined from the surface of the ellipsoid to points lying on the physical surface of the Earth along lines normal to the surface of the ellipsoid containing the points in question (Lamparski, 2001; Misra and Enge, 2002). The fundamental GNSS observations are code pseudorange and carrier phase measurements, described as (Leick, 1995; Hofmann-Wellenhof et al., 2008):

$$\mathrm{P}^s_k = \rho^s_k + \left(\delta t^s - \delta t_k\right)c + \delta\rho_{\mathrm{ion}} + \delta\rho_{\mathrm{trop}} + \varepsilon_P \tag{3}$$

$$\Phi^s_k = \rho^s_k + \lambda N^s_k + \left(\delta t^s - \delta t_k\right)c - \delta\rho_{\mathrm{ion}} + \delta\rho_{\mathrm{trop}} + \varepsilon_\Phi \tag{4}$$

where code pseudorange is denoted as P^s_k, c is the speed of light indices s and k refer to the satellite and GNSS receiver antenna. Phase observation is denoted with Φ^s_k, λ is carrier wavelength. ρ^s_k refers to the geometric distance between satellite and GNSS receiver antenna (Cellmer et al., 2010; Remondi, 1991; Teunnissen, 1995). δt^s and δt_k denote satellite and receiver clock biases, respectively. The ionospheric refraction and tropospheric refraction are represented by $\delta\rho_{\mathrm{ion}}$ and $\delta\rho_{\mathrm{trop}}$. Random errors of the code pseudorange and phase pseudoranges are denoted by ε_P and ε_Φ, and finally N^s_k denotes ambiguity of phase observations.

GNSS leveling is a process that combines a position determined by GNSS measurements, spatially referenced to a specific ellipsoid, and a geoid (quasi-geoid) model developed relative to the same reference ellipsoid. Based on the coordinates of a given point, latitude ϕ and longitude λ, the undulation of the geoid N, expressing the distance of the geoid from the ellipsoid at a given point along the actual plumb line, is interpolated from the geoid model. The orthometric height H^O, representing the height in the real vector field of gravity, is obtained by differentiating the ellipsoidal height h and the undulation of the geoid (Czarnecki, 1997). It can be written as:

$$H^O = h - N\,. \tag{5}$$

When transforming from the orthometric height system to the normal height system, the geoid undulation N can be converted to the height anomaly ζ using the Bouguer anomaly Δg^B (Heiskanen and Moritz, 1981; Kloch and Kryński, 2008). It can be written as:

$$\zeta = N - \frac{\Delta g^B}{\gamma}H^o\,. \tag{6}$$

This makes it possible to express the normal height H^N, i.e. the height in the normal vector field of gravity, where the normal grav-

ity γ is determined, as:

$$H^N = h - \zeta\,. \tag{7}$$

At a given point along a normal vertical line, the height anomaly ζ represents the distance between the Molodensky quasi-geoid and the reference ellipsoid within a Cartesian 3D coordinate system (see Figure 1) (Czarnecki, 1997).

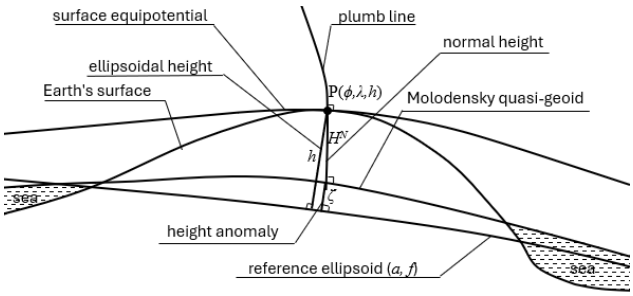

Figure 1. Molodensky quasi-geoid and reference ellipsoid.

Several studies of the quasi-geoid model for Poland have appeared in geodetic studies since the beginning of the 21st century (e.g., leveling geoid 2000, PL-geoid-2011) (Kadaj, 2010; Osada, 2015; Stepniak et al., 2016). The accuracy of these studies has evolved with the availability of new leveling and gravity data, as well as with the increasing accuracy of the realized spatial system, now defined based on permanent GNSS observations collected at ASG-EUPOS stations. The quasi-geoid model now in force in Poland is PL-geoid2021[2], which combines the PL-EVRF2007-NH vertical coordinate system with the PL-ETRF-2000 3D spatial system referenced to the GRS'80 ellipsoid.

4 Static GNSS measurement method on existing vertical network points – solutions

In satellite leveling, a static satellite measurement over the mark of a vertical network involves centering a GNSS antenna, mounted on a surveying tripod, and accurately determining its height over the mark. Next, static GNSS measurements and data processing are performed. Direct, accurate determination of the height of a GNSS antenna is difficult to achieve with a linear gauge, so it is recommended to determine it precisely by indirect methods, such as using a total station, which is problematic to implement and can cause a number of errors. At the University of Warmia and Mazury in Olsztyn, a method of conducting a static measurement on vertical network marks has been developed, using a device for forced precise centering of the GNSS antenna (see Figure 2 (Baryla, 2007)). This solution allows for the determination of the vertical height of the antenna over the vertical point mark with an accuracy of 0.3 mm (at a centering height of 2 m). The height of the Antenna Reference Point (ARP) of the GNSS antenna over the mark is determined directly by the height of the instrument. Bearing in mind that the leveling networks on the territory of Poland were established over several decades, various solutions for the stabilization of ground signs of height points can be observed. Several types of used marks (benchmarks) are used, including cast-iron marks of various sizes, as well as stainless steel benchmarks produced by machining. These signs can be above the ground as well as below it, and the main axis of the mark can be oriented horizontally or vertically. Given the above, it was necessary to develop universal solutions for static GNSS measurements on existing points of a

2 https://www.gov.pl/web/gugik/modele-danych

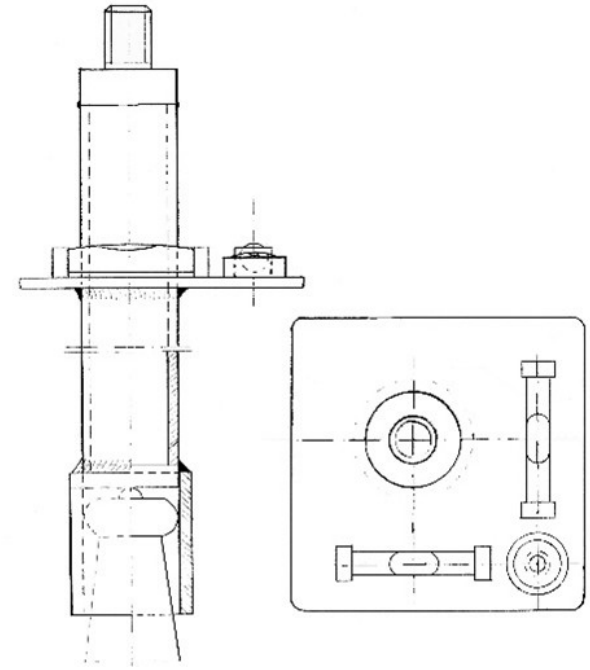

Figure 2. Instrument for precise forced centering of GNSS antennas (Baryla, 2007)

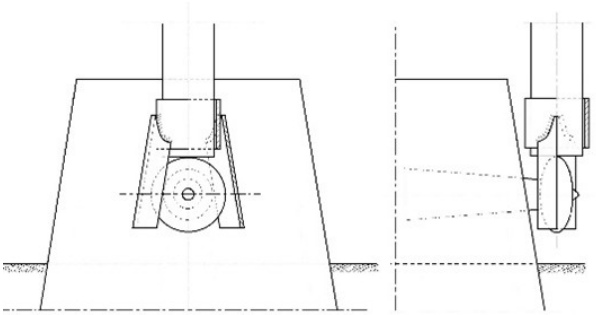

Figure 3. Instrument stabilizer for precise forced centering of GNSS antennas, on vertical marks with horizontal principal axis, especially in precision satellite leveling technique (Baryla, 2025b)

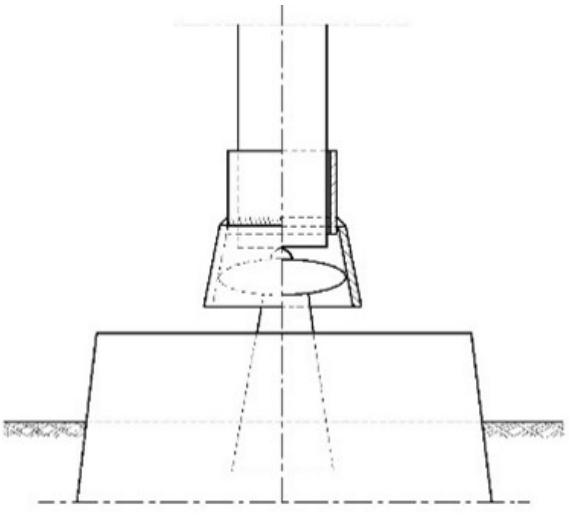

Figure 4. Stabilizer for positioning a GNSS antenna over a vertical point with a vertical benchmark axis (Baryla, 2025a)

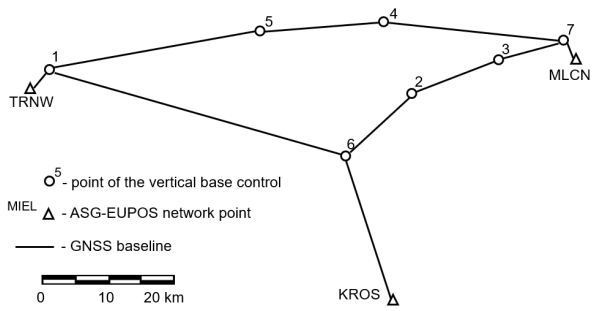

Figure 5. Sketch of GNSS control network

precise leveling network. A triangular head (see Figure 3 (Baryla, 2025b)) can be used to precisely center the instrument on points with a horizontally seated master mark, which stabilizes the instrument regardless of the diameter of that mark. If the main sign is vertically seated, a conical head (see Figure 4 (Baryla, 2025a)) should be used to stabilize the gauge, the size of which should be selected for the type of sign. A conical head designed for a given type of sign (diameter) ensures precise alignment of the gauge within the range of manufacturing accuracy of a given set of signs. Since the height of the gauge was selected with respect to points stabilized on the ground surface, a properly made extension piece of the gauge, with a precisely determined length, should be used for GNSS measurements on underground points.

In satellite positioning, especially in height measurements, the accuracy of the phase center model of the GNSS antennas is crucial. It was proved that GNSS antennas of the same type can exhibit a different position of the mean phase center relative to the antenna model provided by the International GNSS Service (IGS) or National Geodetic Survey (NGS) laboratories (Becker et al., 2010; Dawidowicz, 2017; Stępniak et al., 2015). In order to maintain accuracy in vertical measurements, it is recommended to verify the GNSS antennas before field campaigns. Verification of the GNSS antennas involves conducting long-term measurement sessions on points with known coordinates, followed by post-processing using available GNSS antenna models (Baryła and Dawidowicz, 2024). The resulting differences between the mean phase center and the model should be included.

5 Field tests

Analyses on the performance of the integration of GNSS measurements with precise geometric leveling were conducted on a site located in the Podkarpackie province. A set of 7 points of the vertical base control network was selected: 1, 2, 3, 4, 5, 6, 7, forming a closed polygon consisting of baselines of 11 ÷ 45 km in length (see Figure 5). The points of reference of GNSS satellite measurements to the state 3D system PL-ETRF2000 were the three nearest ASG-EUPOS (Active Geodetic Network – European Position Determination System) network stations: MLCN, KROS, TRNW, which are located around the studied object.

Seven Topcon HiPer VR GNSS receivers were used for the measurement campaign. In order to increase the reliability of the obtained results, two twelve-hour sessions of static GNSS measurements were planned, which were conducted simultaneously at all surveyed points. The following observation parameters were adopted: measurement interval of 1s, elevation mask of 10°, recording of observations from all four available satellite systems, forced precise centering of GNSS antennas using a dedicated instrument (see Figure 6), thus eliminating errors in determining the height of GNSS antennas over the measurement points. Prior to the field measurements, calibration measurements of these instruments were performed in two sessions using a precision code level (Leica DNA03) and an invar staff. The instrument heights were designated as: T_1, T_2, T_3, T_4, T_5, T_6, T_7 (see Table 1).

Table 1. Summary of instrument heights for forced precise centering of GNSS antennas

No	T_1	T_2	T_3	T_4	T_5	T_6	T_7
Height [m]	1.5004	1.5002	1.5003	1.5005	1.5005	1.5005	1.5004

Figure 6. Static GNSS measurement on a vertical network point using an instrument for precise forced centering of the GNSS antenna

An analysis of the shapes of the principal marks of the vertical points, based on the inventory materials, revealed variations in the sizes of the vertical points and their horizontal or vertical stabilization. The existing conditions required the application of new solutions to stabilize the instrument for precise forced centering of GNSS antennas. A triangular head (see Figure 7) was used on vertical point marks with benchmarks with a horizontal axis of orientation, while conical heads were utilized on marks with benchmarks with a vertical axis of orientation (see Figure 8). It should be emphasized that the adoption of the above solutions provides accurate and symmetrical alignment with the benchmark axis regardless of its dimensions and manufacturing accuracy. At the same time, it allows the instrument to move freely under gravity for precise forced centering of the GNSS antenna until it comes into contact with the benchmark extremity. The combination of the above properties with the ability of the instrument to rotate freely in a head placed on a surveying tripod ensures the correct alignment of the GNSS antenna with respect to the north direction, which is a prerequisite for the adoption of precise GNSS antenna models in post-processing.

Static GNSS measurements at the study site were conducted by 7 survey teams in August 2024.

6 Result analysis

Based on the sets of GNSS observations recorded during two 12-hour-long observation sessions and data from the three ASG-EUPOS stations KROS, MLCN, and TRNW, which were closest to the analyzed object (Figure 5), we proceeded to the post-processing

Figure 7. Accurate centering of the instrument for precise forced centering of a GNSS antenna on a benchmark of about 63 mm in diameter with horizontal axis orientation, using a triangular head

Figure 8. Placing the conical head on a benchmark approximately 63 mm in diameter with the axis vertical, before setting up the GNSS antenna precision forced centering device

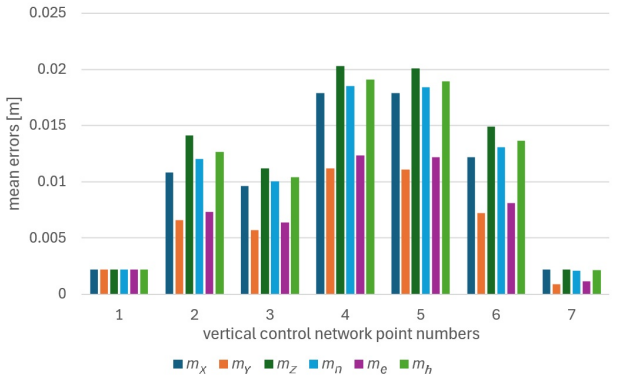

Figure 9. Formal error values of points in the geocentric coordinate system: m_X, m_Y, m_Z, and in the topocentric geodetic system: m_n, m_e, m_h

of the collected measurements. Satellite baselines were computed according to a polygonal sequence (Figure 5), which is key in precise geometric leveling, where the network has the shape of closed meshes. The formation of a closed string is also crucial in the context of the law of error propagation, as it forces the adjustment to obtain a sum of differences in heights equal to zero (Wiśniewski, 2009). This approach also facilitates a direct comparison of the accuracy of differences in heights between neighboring points obtained from satellite leveling, with the heights achieved with geometric leveling measurements (Baryła, 2018; Stepniak et al., 2016). Post-processing was conducted using MAGNET Tools 5.1 software, with the following parameters: GNSS systems — GPS, GLONASS, GALILEO, 10° masking elevation, precise orbits, and clocks, GNSS antenna models — NGS, ionosphere handling — application of ionospheric free linear combination, troposphere handling — Niell model. First, the components of the coordinate baseline were determined. Next, two network adjustments were performed based on GNSS baseline coordinates (Table 2) and assuming standard deviations from square roots of variance, which are elements of the diagonal of the covariance matrix Σ, as accuracy elements: $var(\Delta X)$, $var(\Delta Y)$, $var(\Delta Z)$. The covaraince Σ matrix is given as:

$$\Sigma = \begin{bmatrix} var(\Delta X) & cov(\Delta X, \Delta Y) & cov(\Delta X, \Delta Z) \\ cov(\Delta Y, X) & var(\Delta Y) & cov(\Delta Y, \Delta Z) \\ cov(\Delta Z, \Delta X) & cov(\Delta Z, \Delta Y) & var(\Delta Z) \end{bmatrix}. \quad (8)$$

To conduct the first, free adjustment, baselines were selected between the determined points (Figure 5), while the fixed point was adopted as point No. 3, whose coordinates in the PL-ETRF2000 system were determined earlier with reference to the ASG-EUPOS station. The second adjustment was conducted by attaching baselines to ASG-EUPOS stations and assuming their coordinates as fixed. The maximum values of the mean errors of coordinate components derived from the adjustment of GNSS baselines (see Figure 9) reached m_Z = 20.3 mm for points 4 and 5. After the transformation of Cartesian coordinates to the ellipsoidal system (GRS80), the latitude ϕ, longitude λ, and ellipsoidal heights h of the points were obtained.

The maximum errors of horizontal coordinate errors in the topocentric geodetic system occurred in points 4 and 5: m_n – for the northern component, 18.5 mm, and 18.4 mm, m_e – for the eastern component, 12.4 mm, and 12.2 mm, m_h – for the ellipsoidal height, 19.1 mm, and 18.9 mm.

The maximum accuracy values of horizontal coordinates in the topocentric geodetic system for point No. 4 were m_n = 18.5 mm for the northern component and m_e = 12.4 mm for the eastern component. The point with the largest error in ellipsoidal height m_h = 19.1 mm also turned out to be point No. 4.

The ellipsoidal heights of the points were converted according

Table 2. Summary of GNSS baseline coordinates: ΔX, ΔY, ΔZ, and their variances: $var(\Delta X)$, $var(\Delta Y)$, $var(\Delta Z)$

No. baseline	ΔX [m]	ΔY [m]	ΔZ [m]	$var(\Delta X)$ [m²]	$var(\Delta Y)$ [m²]	$var(\Delta Z)$ [m²]
1 - 5	-14007.702	23910.257	3664.330	0.012	0.007	0.013
1 - 6	-7624.453	44248.811	-7331.034	0.021	0.013	0.017
1 - TRNW	1164.459	-632.692	-692.648	0.001	0.001	0.001
2 - 3	-8338.875	3523.347	5265.558	0.003	0.002	0.006
2 - 6	8773.880	-4748.751	-5320.548	0.004	0.002	0.006
3 - 7	-4587.078	10923.254	140.042	0.005	0.003	0.006
4 - 5	6685.337	-11241.395	-1764.278	0.005	0.003	0.006
4 - 7	-8631.257	28292.473	-2033.506	0.012	0.008	0.014
6 - KROS	14809.646	18533.981	-17502.967	0.013	0.008	0.013
7 - MLCN	630.795	199.454	-532.987	0.001	0.000	0.001

Table 3. Heights of points in the normal height system: catalog heights H^N_C, free adjustment H^N_{A1}, adjustment with reference to ASG-EUPOS H^N_{A2}, height errors of points from adjustment: $m_{H(A1)}$, $m_{H(A2)}$, and height differences adjusted to catalog heights: dH^N_{A1-C}, dH^N_{A2-C}

No.	H^N_C [m]	H^N_{A1} [m]	$m_{H(A1)}$ [mm]	H^N_{A2} [m]	$m_{H(A2)}$ [mm]	dH^N_{A1} [mm]	dH^N_{A2} [mm]
1	218.0502	218.0502	2.1	218.0508	2.1	0.0	0.6
2	332.4100	332.4415	9.1	332.4506	6.1	31.5	40.6
3	232.8911	232.8858	9.1	232.9008	5.2	-5.3	9.7
4	193.0870	193.0908	8.4	193.1071	5.2	3.8	20.1
5	191.1605*	191.1418	7.4	191.1532	5.8	-18.7	-7.4
6	376.7110	376.7371	8.6	376.7349	5.8	26.1	23.9
7	222.5141	222.4886	8.9	222.5095	3.1	-25.5	-4.6
TARN	277.0700	-	-	-	-	-	-
MLCN	271.9930	271.9675	9.5	-	-	-25.5	-
KROS	347.5370	347.5631	12.8	-	-	26.1	-
		Standard deviation σ				19.6**	16.1

* height from GNSS measurements, taking into account height anomaly
** excluding points: MLCN, KROS

to Formula (6) to the network system PL-EVRF2007-NH, based on the quasi-geoid model PL-geoid2021. Model height differences in the normal height system were obtained based on the benchmark height differences of neighboring points. In the case of point No. 5, there was a problem resulting from the lack of catalog height, because the damaged sign had been previously restored. Consequently, the height from GNSS measurements was used for the analysis, including the height anomaly. Next, network adjustment was performed in two variants: A1 – free adjustment, A2 – adjustment in relation to 3 points of the ASG-EUPOS network. Table 3 shows the heights of points: catalog heights H^N_C, averages of two measurement sessions from the free adjustment to point TARN H^N_{A1}, averages of two measurement sessions from the adjustment to the ASG-EUPOS network H^N_{A2} and differences in heights between the results of the first dH^N_{A1-C} and second dH^N_{A2-C} adjustments, respectively, and catalog coordinates.

Analyzing the height differences obtained based on free leveling (A1) and catalog data, random height values can be observed in the range of <-25.5 mm; 31.5 mm>. Based on the second adjustment (A2), the height differences fall within the range <-7.4 mm; 40.6 mm>, which is 10.0 mm smaller than the range obtained from the first adjustment (A1). Thus, it can be concluded that the GRS80 ellipsoid obtained in the free adjustment with the ellipsoid defined by the PL-ETRF2000 system is not parallel, and the results from the free adjustment (A1) can only be used to verify the correctness of the calculation process. Additionally, the results of the second adjustment (A2) show an improvement in the accuracy of determining the heights of points based on the mean m_H errors, whose values for the weakest points of the network improved by over 33%. The differences in point heights obtained from the second adjustment (A2), calculated in the PL-ERTF2000 system tied to the ASG-EUPOS network, indicate a systematic lowering of the height system defined by the geometric leveling network points relative to selected ASG-EUPOS stations. Significant height differences of up to -40.6 mm may indicate reduced accuracy of points determined by precise geometric leveling measurements. The mean error m_p is determined as:

$$m_p = \pm m_v \sqrt{L} \quad [mm] \tag{9}$$

depending on the error m_v of double leveling conducted in both directions and the length of the leveling line L expressed in km,

Table 4. Summary of height differences obtained on the basis of: catalog coordinates, free adjustment (A1), and adjustment constrained by ASG-EUPOS sites (A2), variations in identical height differences from adjustment (A1) and (A2), and catalog height differences: $d\Delta H^N_{A1-C}$, $d\Delta H^N_{A2-C}$, obtained errors: $m_{p(A1)}$, $m_{p(A2)}$, and permissible values of these mean errors m_{pmax}

Line No.	L [km]	ΔH^N_C [m]	ΔH^N_{A1} [m]	ΔH^N_{A2} [m]	$d\Delta H^N_{A1-C}$ [mm]	$d\Delta H^N_{A2-C}$ [mm]	$m_{\Delta H(A1)}$ [mm]	$m_{\Delta H(A2)}$ [mm]	$m_{\Delta H_{max}}$ [mm]
1-5	28	-26.8671	-26.8977	-26.9084	-18.73	-8.0	7.1	5.8	7.9
5-4	13	1.9039	1.9540	1.9490	22.53	27.5	5.2	4.8	5.4
4-7	12	29.4271	29.4024	29.3978	-29.3	-24.7	5.0	4.6	5.2
7-3	11	10.3770	10.3913	10.3972	20.2	14.3	4.8	4.6	5.0
2-3	11	-99.5189	-99.5498	-99.5557	-36.8	-30.9	4.8	4.6	5.0
6-2	21	-44.3010	-44.2843	-44.2956	5.4	16.7	6.3	5.7	6.9
1-6	45	158.6608	158.6841	158.6869	26.1	23.3	8.3	5.9	10.1
Standard deviation σ					24.4	21.9			
Correlation coefficient r					0.973				

connecting adjacent points, which may change the position as a result of the subsidence of markers.

The subsequent analyses were conducted based on the obtained heights of points, creating baselines connecting individual points according to the sketch in Figure 5. Table 4 summarizes the obtained lengths L of the baselines, their height coordinates in the normal height system based on catalog coordinates ΔH^N_C, from free adjustment ΔH^N_{A1} and adjustment with reference to ASG-EUPOS ΔH^N_{A2}. The differences of the identical baselines, $d\Delta H^N_{A1-C}$, $d\Delta H^N_{A2-C}$, were calculated from the vertical gains, and these were taken as mv errors for the calculation of errors based on function (9). To control the permissible values of the errors, $m_{p(A1)}$ and $m_{p(A2)}$, from the first and second adjustments, their maximum values m_{pmax} were calculated based on Formula (9), assuming the accuracy of the double geometric leveling m_v = 1.5 mm (Journal of Laws of the Republic of Poland, 2021).

Analyzing the mean errors $m_{\Delta H(A1)}$ and $m_{\Delta H(A2)}$ of the adjusted leveling lines, it can be concluded that they all fall within the acceptable ranges of $m_{\Delta Hmax}$. In the case of adjustment (A2) in relation to 3 points of the ASG-EUPOS network, there is a significant improvement in the accuracy of the results obtained. The lowest accuracy occurred in the case of baseline 1-6 with a length of 45 km. Comparing the height differences obtained from the catalog data with the height differences from free leveling $d\Delta H^N_{A1-C}$ <-30.8 mm; 26.1 mm> and the adjustment in relation to ASG-EUPOS $d\Delta H^N_{A2-C}$ <-30.9 mm; 27.5 mm>, a high correlation can be observed based on the correlation coefficient r = 0.973. The high correlation of the obtained height differences confirms the convergence of the PL-geoid2021 quasi-geoid model with the heights of the ASG-EUPOS network points. The values of height differences $d\Delta H^N_{A1-C}$ and $d\Delta H^N_{A2-C}$, reaching six times the maximum mean error $m_{\Delta Hmax}$ in the case of the 2-3 levelling line are significant. It is assumed that these values may primarily result from outdated catalog heights, derived from precise leveling measurements conducted in 1999–2002, as well as from post-measurement movements of the Earth's surface (Kowalczyk et al., 2020) and the settlement of height control points.

7 Conclusion

The coupling of the GNSS measurements and precise geometric leveling requires a combination of two different height systems. The results of satellite measurements, determined in the Cartesian system, can be presented in the form of ellipsoidal coordinates: latitude, longitude, and height. In contrast, the results of precise geometric leveling are determined in the vector field of the Earth's gravity and are not geometric. The integration of these differently defined coordinate systems is only possible based on a geoid model linking these systems. Currently in Poland, such an official model is the quasi-geoid PL-geoid2021.

Conducting satellite measurements requires the surveyor to accurately determine the height of the GNSS antenna above the geodetic point mark. It is known from experience that this procedure is a source of many errors, especially directly affecting the accuracy of the vertical coordinate, which is important in precise leveling. Therefore, in the GNSS survey procedure at the field site, when integrating satellite with precise geometric leveling, it is recommended to use instruments for precise forced centering of GNSS antennas (depicted in Figures 2 and 6).

Precise leveling networks created over centuries have created a variety of shapes and sizes of the main vertical marks (benchmarks) used in these networks, which could significantly limit the use of instruments for precise forced centering of GNSS antennas, also providing long-term stability of GNSS antennas during static satellite measurements. This problem was solved by using an instrument stabilizer for precise forced centering of GNSS antennas, on vertical network marks with a horizontal principal axis (depicted in Figures 3 and 7) and a stabilizer for positioning the GNSS antenna over a vertical point with a vertical benchmark axis (depicted in Figures 4 and 8).

Based on the results of the presented research, it can be concluded that static satellite measurements fulfil the accuracy requirements in the process of their integration with precise geometric leveling. Baselines of satellite measurements should be used in the fusion, including height anomalies determined based on a suitable, accurate geoid model. The geoid model (quasi-geoid PL-geoid2021), which must integrate the current spatial geocentric coordinate system (PL-ETRF-2000) and the applicable vertical system (PL-EVRF2007-NH), meets the requirements of millimeter accuracy.

References

Barlik, M. and Pachuta, A. (2007). *Geodezja fizyczna i grawimetria geodezyjna: Teoria i praktyka (Physical geodesy and geodetic gravimetry: Theory and practice)*. Oficyna Wydawnicza Politechniki Warszawskiej.

Baryla, R. (2007). Przyrząd do precyzyjnego wymuszonego centrowania anteny GPS. Świadectwo ochrony wzoru użytkowego nr 64831 (A device for the precise forced centering of a GPS an-

tenna. Utility model certificate No. 64831).

Baryła, R. (2018). *Integracja niwelacji geometrycznej z pomiarami satelitarnymi w badaniach nad antropogenicznymi deformacjami powierzchni Ziemi (Integration of geometric leveling with satellite measurements in research on anthropogenic deformations of the Earth's surface)*. Wydawnictwo Uniwersytetu Warmińsko-Mazurskiego w Olsztynie.

Baryla, R. (2025a). Stabilizator do ustawiania anteny GNSS nad punktem wysokościowych z pionową osią reperu. Świadectwo ochrony wzoru użytkowego nr 73906 (A stabilizer for positioning a GNSS antenna above a bench mark with a vertical axis. Utility model registration certificate No. 73906).

Baryla, R. (2025b). Stabilizator przyrządu do precyzyjnego, wymuszonego centrowania anten GNSS, na znakach wysokościowych z poziomą osią główną, zwłaszcza w technice precyzyjnej niwelacji satelitarnej. Świadectwo ochrony wzoru użytkowego nr 73818 (A stabilizer for precise, forced centering of GNSS antennas on bench marks with a horizontal main axis, particularly in the field of precise satellite leveling. Utility model registration No. 73818).

Baryła, R. and Dawidowicz, K. (2024). Analysis of Comparability of PCV in Surveying-Grade GNSS Antenna – Topcon HIPER-VR Case Study. *Artificial Satellites*, 59(3):87–99, doi:10.2478/arsa-2024-0007.

Becker, M., Zeimetz, P., and Schönemann, E. (2010). Anechoic chamber calibrations of phase center variations for new and existing GNSS signals and potential impacts in IGS processing. In *IGS workshop, 28 June – 2 July 2010, Newcastle upon Tyne, England*.

Cellmer, S., Wielgosz, P., and Rzepecka, Z. (2010). GNSS Carrier Phase Processing Using Some Properties of Ambiguity Function Method. In *FIG Congress 2010, Sydney, Australia*.

Czarnecki, K. (1997). *Geodezja współczesna w zarysie (An Overview of Modern Geodesy)*. Wydawnictwo Wiedza i Życie SA.

Dawidowicz, K. (2017). Differences in GPS coordinate time series resulting from the use of individual instead of type-mean antenna phase center calibration model. *Studia Geophysica et Geodaetica*, 62(1):38–56, doi:10.1007/s11200-016-0630-1.

Gajderowicz, I. (2007). Proposal of new Polish vertical reference frame. *Geomatics and Environmental Engineering*, 1(1/1):125–132.

Heiskanen, W. A. and Moritz, H. (1981). *Physical geodesy*. Institute of Physical Geodesy, Technical University, Graz, Austria.

Hofmann-Wellenhof, B., Lichtenegger, H., and Wasle, E. (2008). *GNSS—global navigation satellite systems: GPS, GLONASS, Galileo, and more*. Springer.

Journal of Laws of the Republic of Poland (2021). Regulation of the Minister of Development, Labour and Technology dated 6 July 2021 regarding geodetic, gravimetric, and magnetic networks. Journal of Laws of the Republic of Poland, 2021, item 1341.

Journal of the European Union (2010). Commission Regulation (EU) No. 1089/2010, of November 23, 2010, implementing Directive 2007/2/EC of the European Parliament and of the Council as regards interoperability of spatial data sets and services. Journal of the European Union, No. 323 p. 11, Brussels.

Kadaj, R. (2010). Algorytm opracowania modelu PL-geoid-2011 (Algorithm for developing the PL-geoid-2011 model). In *Implementation of Geodetic Frameworks and Geodynamic Issues, Committee on Geodesy of the Polish Academy of Sciences and Department of Geodesy and Cartography Warsaw University of Technology, September 25–27, 2012, Grybów, Poland*.

Kadaj, R. (2018). Transformations between the height reference frames: Kronsztadt'60, PL-KRON86-NH, PL-EVRF2007-NH. *Czasopismo Inżynierii Lądowej, Środowiska i Architektury*, 65(3):5–24, doi:10.7862/rb.2018.38.

Kamela, C., Warchałowski, E., Włoczewski, F., and Wyrzykowski, T. (1993). *Teoria geometrycznej niwelacji precyzyjnej. Praca zbiorowa – Niwelacja precyzyjna (The Theory of Geometric Precision Leveling – Precision Leveling)*. Polskie Przedsiębiorstwo Wydawnictw Kartograficznych, Warszawa.

Kloch, G. and Kryński, J. (2008). Implementacja długo-, średnio-i krótkofalowych składowych sygnałów funkcjonałów potencjału zakłócającego w procesie modelowania geoidy (Implementation of the long-, medium-, and short-wavelength components of the disturbance potential's functional signals in the geoid modeling process). *Prace Instytutu Geodezji i Kartografii*, 54:5–25.

Kowalczyk, K., Kowalczyk, A. M., and Chojka, A. (2020). Modeling of the Vertical Movements of the Earth's Crust in Poland with the Co-Kriging Method Based on Various Sources of Data. *Applied Sciences*, 10(9):3004, doi:10.3390/app10093004.

Lamparski, J. (2001). *NAVSTAR GPS: od teorii do praktyki (NAVSTAR GPS: From Theory to Practice)*. Wydaw. Uniwersytetu Warmińsko-Mazurskiego.

Leick, A. (1995). *GPS Satellite Surveying*. John wiley and Sons, New York.

Misra, P. and Enge, P. (2002). Global positioning system: Signals, measurements, and Performance. *IEEE aerospace and electronic systems magazine*, 17(10):36–37, doi:10.1109/MAES.2002.1044515.

Ogrodniczak, M., Łyszkowicz, A., Kowalczyk, K., Olszak, T., Czyża, S., and Szuniewicz, K. (2022). Projekt techniczny "Opracowanie projektu modernizacji podstawowej osnowy geodezyjnej wysokościowej na obszar kraju" (Technical Project: "Development of a Plan for the Modernization of the National Basic Geodetic Height Reference System"). Technical report, Olsztyn: SKB GIS s.c.

Osada, E. (2015). Opracowanie quasigeoidy LGOM-2015 (Development of the LGOM-2015 Quasigeoid). Technical report, Sprawozdanie z realizacji umowy z KGHM CUPRUM Centrum Badawczo-Rozwojowe we Wrocławiu, Uniwersytet Przyrodniczy we Wrocławiu, Wrocław.

Remondi, B. W. (1991). Pseudo-kinematic GPS results using the ambiguity function method. *Navigation*, 38(1):17–36, doi:10.1002/j.2161-4296.1991.tb01712.x.

Stepniak, K., Baryla, R., Paziewski, J., Golaszewski, P., Wielgosz, P., Kurpinski, G., and Osada, E. (2016). Validation of regional geoid models for Poland: Lower Silesia case study. *Acta Geodynamica et Geomaterialia*, page 93–100, doi:10.13168/agg.2016.0031.

Stępniak, K., Wielgosz, P., and Baryła, R. (2015). Field tests of L1 phase centre variation models of surveying-grade GPS antennas. *Studia Geophysica et Geodaetica*, 59(3):394–408, doi:10.1007/s11200-014-0250-6.

Teunnissen, P. J. G. (1995). The least-square ambiguity decorrelation adjustment: A method for fast GPS integer ambiguity estimation. *Journal of Geodesy*, 70(1):65–82, doi:10.1007/BF00863419.

Wiśniewski, Z. (2009). *Rachunek wyrównawczy w geodezji (z przykładami) (Adjustment in geodesy (with examples))*. Wydawnictwo Uniwersytetu Warmińsko-Mazurskiego.

Wyrzykowski, T. (1993). Rys historyczny podstawowej osnowy wysokościowej w Polsce (A Brief History of the Basic Vertical Control Network in Poland). *Niwelacja precyzyjna*, pages 491–526.